DYNAMIC MODELLING OF THE CRANK MECHANISM AND HYDRODYNAMIC BEARINGS OF INTERNAL COMBUSTION ENGINES

Rodrigo C. Gerardin
DPM/FEM/UNICAMP, P.O. Box 6051, Campinas/SP, 13083-970, Brazil
rcgerardin@fem.unicamp.br

Fabiano L. M. de Oliveira
DPM/FEM/UNICAMP, P.O. Box 6051, Campinas/SP, 13083-970, Brazil
marquezi@fem.unicamp.br

Marco L. Bittencourt
DPM/FEM/UNICAMP, P.O. Box 6051, Campinas/SP, 13083-970, Brazil
mlb@fem.unicamp.br

Ilmar F. Santos
Denmark Technical University
ifs@mek.dtu.dk

Abstract. *Due to technical, environmental and performance requirements, internal combustion engines must operate with higher combustion pressures. The engine parts shall be optimized to support these requirements as well the lubrication system. The scope of the present work is to develop a mathematical model to determine the dynamic forces in the hydrodynamic bearings of internal combustion engines. For that purpose, the dynamics of one-cylinder has been developed which includes the main crankshaft bearing and the small and big connecting-rod bearings. The Reynolds equations of the hydrodynamic bearings have been solved by the Finite Element Method (FEM). The equations are solved by the Newton-Raphson iterative procedure for a complete engine cycle. The kinematics and dynamic loads are calculated for a constant rotation of the crankshaft. Results are presented to validate the model.*
Keywords: *Hydrodynamic bearings, Crank system dynamics, Reynolds equation, Newton-Raphson method, Finite Element Method.*

1. Introduction

Due to technical, environmental, legislation and performance requirements, internal combustion engines have had to operate with higher combustion pressures. Because of that, lubrication is very important and it is desirable to know the oil pressure and flow in any point of the lubrication circuit of the engine. For that purpose, it is necessary to calculate the dynamic forces in the engine bearings along the engine cycle.

The traditional approach to calculate the dynamic forces is to decompose the inertia force of one cylinder as the sum of oscillatory and rotating inertia forces [1]. Based on that, the forces acting in the bearings may be calculated and the correspondent hydrodynamic pressures are determined by the solution of the Reynolds equations. This means that the forces are calculated for a pinned system and bearing pressures that result in those forces are calculated.

In fact, it is the movement of the piston-conrod-crank elements that generate the pressures in the bearings and after integration the real forces are determined. This approach is considered in this paper. The pressures are determined from the finite element solution of the Reynolds equations. The tangential and normal velocity components of the independent term of the Reynolds equations come from the dynamics of the piston-conrod-crank system. The detailed presentation of the dynamic model is in [4].

Before presenting the model considered in this paper, a brief overview of the literature is considered.

Boneau and Grente (1999) [3] presented a formulation to optimize the elasto-hydrodynamic main bearings in internal combustion engines. The Finite Element Method was used to solve the lubrication problem. A flexible model to analyze the structural behavior of internal combustion engines, which considers the hydrodynamic lubrication on the main bearings, was presented by Mourelatos [9]. The Reynolds equation were also solved by the FEM and the results compared to experimental tests. Zheng-Dong and Perkins (2002) [5] studied an optimized model for the crank system mechanism using Multiple Body Dynamics and hydrodynamic lubrication. Makino and Koga [7] presented a 3D model of the hydrodynamic lubrication of the main bearing of four-stroke engines. They used the FEM and Newton-Raphson method to solve the problem.

A crankshaft model was presented by Mendes [8] for high power diesel engines. The crank system mechanism was studied, considering the inertia and combustion loads and vibrations of the crankshaft and neglecting the hydrodynamic lubrication. Ma and Perkins [6] presented the kinematics of the crank system and solution of the Reynolds equations.

Analysis of rigid and elasto-hydrodynamic bearings of the conrod considering the inertia loads for high speeds was developed in [11].

The paper is organized as follows. First the kinematics of the piston-conrod-crank mechanism is presented. After that, free-body diagrams of the elements are considered and the equilibrium equations are determined. The system of equations obtained from the kinematics and dynamics of the systems is presented. The Reynolds equations and velocity components are considered. Finally, results for a pinned system is considered to illustrate the application of the dynamic model.

2. Kinematics

Fig. 1(a) shows the piston-conrod-crank system. The main, small end and big end bearings are indicated by the letters O, A and B, respectively. Due to the hydrodynamic lubrication, the elements of the system can displace, as illustrated in Fig. 1(a). Thus, the the crankshaft displaces to *O*' and the small and big end connecting rod displace to *A*' and *B*' respectively. In addition, the connecting rod can rotate rigidly of the β_b angle.

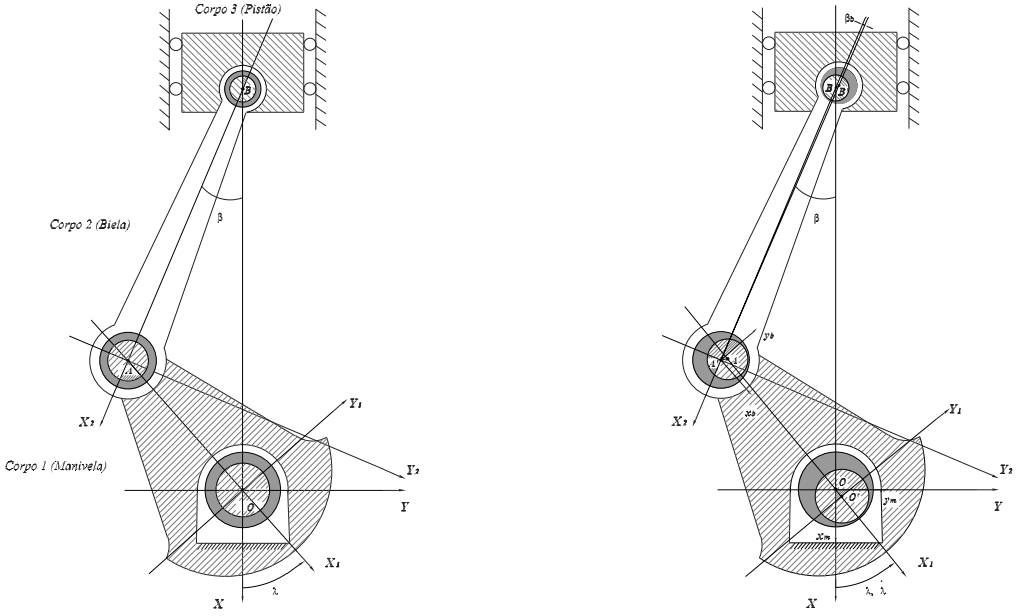

(a) Initial position. (b) Displaced position.

Figure 1. Piston-conrod-crank system.

The crankshaft angle is λ and the respective angular velocity $\dot{\lambda}$ is considered constant. The connecting rod angle and angular velocity are β and $\dot{\beta}$, respectively.

The inertial reference system (X, Y) and the two local coordinates systems B_1 (X_1, Y_1) and B_2 (X_2, Y_2) are also indicated in Fig. 3. The transformation matrices between the inertial and local systems are given by

$$\mathbf{T}_\lambda = \begin{bmatrix} \cos\lambda & \sin\lambda & 0 \\ -\sin\lambda & \cos\lambda & 0 \\ 0 & 0 & 1 \end{bmatrix} => {}_{B1}\mathbf{s} = \mathbf{T}_\lambda \, {}_I\mathbf{s},$$

$$\mathbf{T}_{(\beta+\beta_b)} = \begin{bmatrix} \cos(\beta+\beta_b) & -\sin(\beta+\beta_b) & 0 \\ \sin(\beta+\beta_b) & \cos(\beta+\beta_b) & 0 \\ 0 & 0 & 1 \end{bmatrix} => {}_{B2}\mathbf{s} = \mathbf{T}_{(\beta+\beta_b)} \, {}_I\mathbf{s}.$$

The system kinematics is illustrated in Fig. 2 and the following vectorial equation is valid

$${}_I\mathbf{r}_{OB} + {}_I\mathbf{dp} + \mathbf{T}^T_{(\beta+\beta_b)} \, {}_I\mathbf{d}\beta_b + \mathbf{T}^T_{(\beta+\beta_b)B2}\mathbf{L} + \mathbf{T}^T_{\lambda B1}\mathbf{db} + \mathbf{T}^T_{\lambda B1}\mathbf{r} + {}_I\mathbf{dm} = \mathbf{0}. \tag{1}$$

The vectors **dm**, **db** and $\mathbf{r}_b$ are, respectively, the crankshaft, big end and small end displacements; $\mathbf{r}_b$=**dp** + $\mathbf{d}\beta_b$; **dp** is the piston displacement; and $\mathbf{d}\beta_b$ is the conrod rigid rotation. Considering β_b small, the displacement $\mathbf{d}\beta_b$ is in the $-Y_2$ direction and its module is Lβ_b, where L is the length of the connecting rod.

Applying the transformation matrices, equation (1) assumes the final form

$$\begin{Bmatrix} -r_{OB} \\ 0 \\ 0 \end{Bmatrix} + \begin{Bmatrix} -x_p \\ 0 \\ 0 \end{Bmatrix} + \begin{Bmatrix} -L\beta_b \sin(\beta+\beta_b) \\ -L\beta_b \cos(\beta+\beta_b) \\ 0 \end{Bmatrix} + \begin{Bmatrix} L\cos(\beta+\beta_b) \\ -L\sin(\beta+\beta_b) \\ 0 \end{Bmatrix} +$$

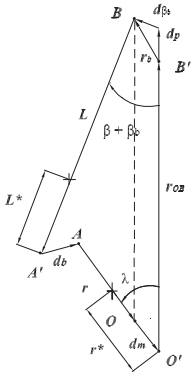

Figure 2. System kinematics.

$$\left\{ \begin{array}{c} x_b \cos\lambda - y_b \sin\lambda \\ x_b \sin\lambda + y_b \cos\lambda \\ 0 \end{array} \right\} + \left\{ \begin{array}{c} r\cos\lambda \\ r\sin\lambda \\ 0 \end{array} \right\} + \left\{ \begin{array}{c} x_m \\ y_m \\ 0 \end{array} \right\} = \left\{ \begin{array}{c} 0 \\ 0 \\ 0 \end{array} \right\}, \tag{2}$$

where r_{OB}, x_p, β, β_b, x_b, y_b, x_m and y_m are the unknown variables. Differentiating twice the previous equation and as $\ddot{\lambda} = 0$, the terms related to the unknown accelerations $\ddot{r}_{OB}$, $\ddot{x}_p$, $\ddot{\beta}$, $\ddot{\beta}_b$, $\ddot{x}_b$, $\ddot{y}_b$, $\ddot{x}_m$ and $\ddot{y}_m$ are obtained.

3. Dynamics

Fig. 3 presents the free body diagrams for the crank, connecting rod and piston. The crank and connecting rod are considered rigid bodies and the piston is a particle [10]. The Newton-Euler method was used to determine the dynamic loads of the system as follows.

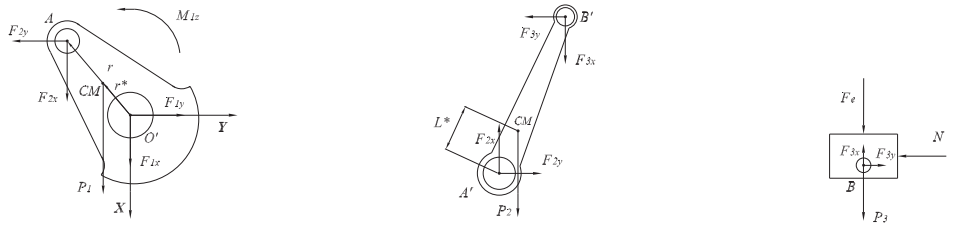

(a) Body 1: crank. (b) Body 2: conrod. (c) Body 3: piston.

Figure 3. Free body diagrams.

- Body 1 (crank) - it has mass m_1 and is loaded by its weight ($\mathbf{P}_1$), the main bearing forces ($\mathbf{F}_1$), the connecting rod forces ($\mathbf{F}_2$) and the moment ($\mathbf{M}_1$). The force $\mathbf{F}_2$ are represented in the local system *B1*, because the displacement components (x_b,y_b) are defined in the *B1* coordinate system.

  The Newton's second law with the vectors represented in the inertial system is applied and

$$\sum_{i=1}^{3} {}_I\mathbf{F}_i = m_1\ {}_I\mathbf{a}_1^* \ \Rightarrow \ \left\{ \begin{array}{c} m_1 g \\ 0 \\ 0 \end{array} \right\} + \mathbf{T}_\lambda^T \left\{ \begin{array}{c} F_{2x} \\ -F_{2y} \\ 0 \end{array} \right\} + \left\{ \begin{array}{c} F_{1x} \\ F_{1y} \\ 0 \end{array} \right\} = m_1 \left\{ \begin{array}{c} a_{1x}^* \\ a_{1y}^* \\ 0 \end{array} \right\}, \tag{3}$$

  where ${}_I\mathbf{a}_1^*$ is the acceleration of the center of mass in the inertial system. Taking the point *O'* as the reference, that acceleration is given by

$${}_I\mathbf{a}_1^* = {}_I\ \mathbf{a}_{O'} + {}_I\,\omega_1 \times ({}_I\omega_1 \times {}_I\mathbf{r}^*) + {}_I\,\dot{\omega}_1 \times {}_I\mathbf{r}^* + 2\,{}_I\dot{\omega}_1 \times {}_I\mathbf{v}_{rel} + {}_I\mathbf{a}_{rel}.$$

  In the previous equation, ${}_I\mathbf{a}_{O'} = {}_I\ddot{\mathbf{dm}}$ and ${}_I\mathbf{r}^*$ is the distance from *O'* to the center of mass (Fig. 3(a)). The term related to $\ddot{\lambda}$ is neglected, because $\ddot{\lambda} = 0$. As the body is rigid, the distance between *O'* and the center of mass is constant and consequently ${}_I\mathbf{v}_{rel}$ = **0** and ${}_I\mathbf{a}_{rel}$ = **0**. Therefore,

$${}_I\mathbf{a}_1^* = \left\{ \begin{array}{c} a_{1x}^* \\ a_{1y}^* \\ 0 \end{array} \right\} = \left\{ \begin{array}{c} \ddot{x}_m \\ \ddot{y}_m \\ 0 \end{array} \right\} + \left\{ \begin{array}{c} \dot{\lambda}^2 r^* \cos\lambda \\ \dot{\lambda}^2 r^* \sin\lambda \\ 0 \end{array} \right\}. \tag{4}$$

The Euler's equation in the base *B1* related to the point *O'* is

$$\sum_{i=1}^{2} {}_{B1}\mathbf{M}_{O'i} = \underbrace{{}_{B1}\mathbf{I}_{O'}\,\frac{d}{dt}({}_{B1}\dot{\lambda})}_{=0} + \underbrace{{}_{B1}\dot{\lambda}\times({}_{B1}\mathbf{I}_{O'}\,{}_{I}\dot{\lambda})}_{=0} + {}_{B1}\mathbf{r}^{*}\times m_1\,{}_{B1}\mathbf{a}_{O'}$$
$$= {}_{B1}\mathbf{r}\times{}_{B1}\mathbf{F}_2 + {}_{B1}\mathbf{r}^{*}\times{}_{B1}\mathbf{P}_1 + {}_{B1}\mathbf{M}_1, \tag{5}$$

where ${}_{B1}\mathbf{r} = \left\{\begin{array}{ccc} r & 0 & 0 \end{array}\right\}^T$ is the distance between points *O'* and *A* (Fig. 3(a)). The second term of the right side is zero because the angular velocities of the body and system $B1$ are equal.

- Body 2 (connecting rod) - it has mass m_2 and is loaded by its weight ($\mathbf{P}_2$) and big ($\mathbf{F}_2$) and small end ($\mathbf{F}_3$) forces.

  The Newton's second law, with the vectors represented in the inertial system, gives

$$\sum_{i=1}^{3} {}_{I}\mathbf{F}_i = m_2\,{}_{I}\mathbf{a}_2^{*} \;=>\; \left\{\begin{array}{c} m_2 g \\ 0 \\ 0 \end{array}\right\} + \mathbf{T}_{\lambda}^{T}\left\{\begin{array}{c} -F_{2x} \\ F_{2y} \\ 0 \end{array}\right\} + \left\{\begin{array}{c} F_{3x} \\ -F_{3y} \\ 0 \end{array}\right\} = m_2\left\{\begin{array}{c} a_{2x}^{*} \\ a_{2y}^{*} \\ 0 \end{array}\right\}, \tag{6}$$

  where ${}_{I}\mathbf{a}_2^{*}$ is the acceleration of the center of mass of the connecting rod indicated by $\mathbf{L}^{*}$ in Fig. 3(b). It is defined in the inertial system as

$${}_{I}\mathbf{a}_2^{*} = {}_{I}\,\mathbf{a}_{A'} + {}_{I}\,\omega_2\times({}_{I}\omega_2\times{}_{I}\,\mathbf{L}^{*}) + {}_{I}\,\ddot{\omega}_2\times{}_{I}\,\mathbf{L}^{*} + 2\,{}_{I}\omega_2\times{}_{I}\,\mathbf{v}_{rel} + {}_{I}\,\mathbf{a}_{rel}.$$

  As points *A'* and L^{*} belong to the same rigid body, it is concluded that ${}_{I}\mathbf{v}_{rel}$ = 0 and ${}_{I}\mathbf{a}_{rel}$ = 0. From the kinematics

$${}_{I}\mathbf{a}_{A'} = {}_{I}\mathbf{a}_{A} + \mathbf{T}_{\lambda\,B1}^{T}\ddot{\mathbf{db}} = {}_{I}\mathbf{a}_{O'} + {}_{I}\,\omega_1\times({}_{I}\omega_1\times{}_{I}\mathbf{r}^{*}) + \mathbf{T}_{\lambda\,B1}^{T}\ddot{\mathbf{db}}.$$

  The application of the Euler's equation based on the point *A'* results

$$\sum_{i=1}^{1} {}_{B2}\mathbf{M}_{A'i} = {}_{B2}\mathbf{I}_{A'}\frac{d}{dt}(\dot{\beta}+\dot{\beta}_b) + \underbrace{{}_{B2}(\dot{\beta}+\dot{\beta}_b)\times[{}_{B2}\mathbf{I}_{A'\,B2}(\dot{\beta}+\dot{\beta}_b)]}_{=0} +$$
$${}_{B2}\mathbf{L}^{*}\times m_2\,{}_{B2}\mathbf{a}_{A'} = {}_{B2}\mathbf{L}\times{}_{B2}\mathbf{F}_3 + {}_{B2}\mathbf{L}^{*}\times{}_{B2}\mathbf{P}_2. \tag{7}$$

- Body 3 (piston) - it has mass m_3 and is loaded by its weight $\mathbf{P}_3$, bearing forces $\mathbf{F}_3$, normal force $\mathbf{N}$ and explosion force $\mathbf{F}_e$, as shown in Fig. 3(c).

  Applying the Newton's second law results

$$\sum_{i=1}^{4} {}_{I}\mathbf{F}_i = m_3\,{}_{I}\mathbf{a}_3 \;=>\; \left\{\begin{array}{c} m_3 g \\ 0 \\ 0 \end{array}\right\} + \left\{\begin{array}{c} -F_{3x} \\ F_{3y} \\ 0 \end{array}\right\} + \left\{\begin{array}{c} 0 \\ -N \\ 0 \end{array}\right\} + \left\{\begin{array}{c} F_e \\ 0 \\ 0 \end{array}\right\} = m_3\left\{\begin{array}{c} {}_{I}a_{3x} \\ 0 \\ 0 \end{array}\right\}. \tag{8}$$

  It is observed that ${}_{I}\mathbf{a}_3 = -(\ddot{\mathbf{r}}_{OB} + \ddot{\mathbf{dp}})$, because the piston acceleration is on the vertical direction X.

3.1 System of Equations

The total number of equations of the system is 16. But there are only 10 equations (two equations from the kinematics and the eight equilibrium equations from the dynamics of the system). The solution of the Reynolds equations for the hydrodynamic bearings O, A and B result in the forces F_{ix} and F_{iy} (i=1,2,3). This reduces the number of unknowns to 10 and make the system of equations determined. Based on that, the following non-linear system of equations must be solved to determine the 10 unknowns

$$\left[\begin{array}{cc} A & B \\ C & D \end{array}\right]\left\{\begin{array}{c} \zeta \\ \eta \end{array}\right\} = \left\{\begin{array}{c} \kappa \\ \iota \end{array}\right\},$$

where

$$\zeta = \left\{\begin{array}{ccccccccc} \ddot{x}_m & \ddot{y}_m & \ddot{x}_b & \ddot{y}_b & \ddot{x}_p & \ddot{\beta}_b & N & M_{1z} & \ddot{r}_{OB} & \ddot{\beta} \end{array}\right\}^T,$$
$$\eta = \left\{\begin{array}{cccccc} F_{1x} & F_{1y} & F_{2x} & F_{2y} & F_{3x} & F_{3y} \end{array}\right\}^T.$$

As η is known, the previous equation is written as

$$[\ A\ ]\{\ \zeta\ \} = \{\ \kappa\ \} - [\ B\ ]\{\ \eta\ \}. \tag{9}$$

The system of equations (9) is non-linear, because the coefficients are dependent of β_b and $\dot{\beta}_b$, which are obtained by integrations of $\ddot{\beta}_b$. The Newton-Rapshon method [2] is used for the solution of (9). It is necessary to solve the following system of equations iteratively

$$[\ A\ ]\{\ \Delta\zeta\ \} = \{\ \phi\ \}, \tag{10}$$

where $\{\ \phi\ \}$ the residue vector.

4. Reynolds Equation and Velocity Components

Fig. 4 shows the geometry of the bearing. The mathematical model is developed considering the coordinate system *XYZ* on the bearing center *O* and the angular coordinate θ.

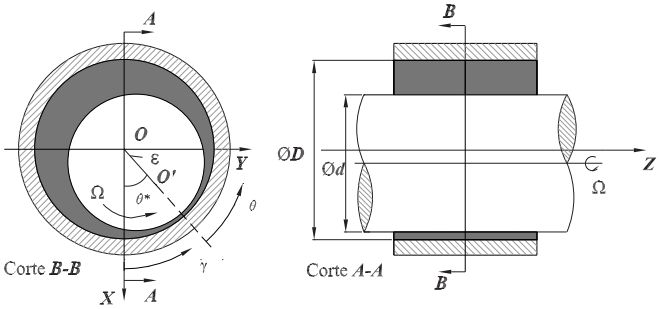

Figure 4. Vistas em corte transversal (**B-B**) e corte longitudinal (**A-A**).

The Reynolds equation is given by

$$\frac{1}{r_J^2}\frac{\partial}{\partial}\left(h^3\frac{\partial P}{\partial\theta}\right) + \frac{\partial}{\partial z}\left(h^3\frac{\partial P}{\partial z}\right) = 6\mu\Omega r_J\frac{\partial h}{\partial\theta} - 12\mu\frac{\partial h}{\partial t}, \tag{11}$$

where μ and h are the the oil viscosity and oil film thickness, respectively. The tangential sliding velocity is $U = \Omega r$ and corresponds to the oil film shear effect. The normal squeeze velocity is given by the term $\frac{\partial h}{\partial t}$.

For the main bearing, the terms $\frac{dh_1}{dt}(\dot{x}_m, \dot{y}_m)$ and U_1 are obtained, respectively, as

$$U_1 = r_{J1}\dot{\lambda},$$

$$\frac{dh_1}{dt} = \frac{d}{dt}\,(h_{01}\ -\ |\varepsilon_{\mathbf{1}}|\cos\theta),$$

where r_1 is the crankshaft major radius and h_{01} the initial oil film thickness. The equilibrium position of the rotor is defined by the eccentricity ${}_I\varepsilon_{\mathbf{1}} = {}_I\mathbf{dm} = \{\ x_m \quad y_m \quad 0\ \}^T$ and the attitude angle $\theta_1^* = \sin^{-1}\frac{x_m}{|\varepsilon_{\mathbf{1}}|}$; θ is the angular coordinate with origin in the X axis as shown in Fig. 5(a).

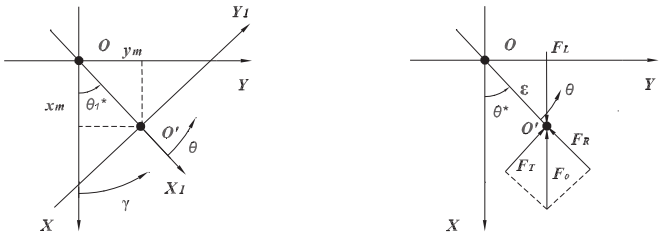

(a) θ and θ_1^*. (b) Static equilibrium.

Figure 5. Main bearing.

The evaluation of the Reynolds equation results in the main bearing pressure P_1. The integration of the oil pressure gives the force in the bearing. The radial F_{iR} and tangential F_{iT} components ($i = 1, 2, 3$), may be evaluated by the following integrals

$$\begin{cases} F_{Ri} = 2\displaystyle\int_0^{L/2}\int_0^{2\pi} P_i R\cos\theta d\theta dz, \\ F_{Ti} = 2\displaystyle\int_0^{L/2}\int_0^{2\pi} P_i R\sin\theta d\theta dz. \end{cases}$$

Therefore, the resultant force in the bearing, F_i, is given by
$F_i = \sqrt{{F_{Ri}}^2 + {F_{Ti}}^2}$.

To obtain the components F_{ix} and F_{iy} of the inertial system is necessary to describe the radial and tangential components on the cartesian system.

The tangential and squeeze velocities for the conrod bearings may be determined analogously [4].

5. Results

The presented model was used to obtain the dynamic forces in one-cylinder of an internal combustion engine. The crankshaft is driven at the constant speed of 2200 rpm and loaded by the combustion pressure curve given in Fig. 6(a). The piston diameter, the conrod length and the crank radius are dp=85.5 mm, L=175.4 mm and r=58.7 mm, respectively. The results were obtained considering pinned bearings and were compared with the software AVL/Excite. Fig. 6 presents the vertical force components on the bearings.

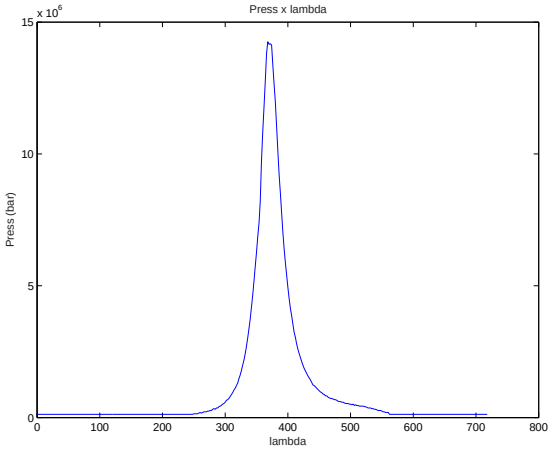

(a) Pressure curve.

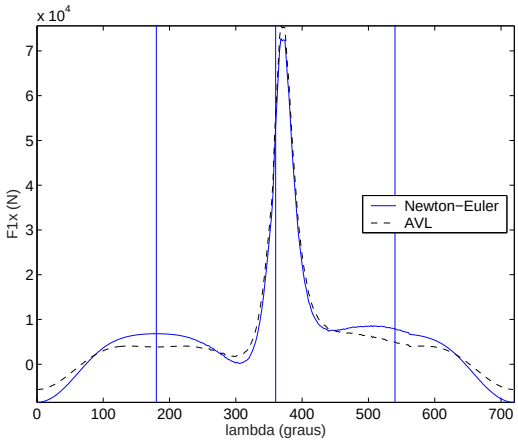

(b) Main bearing.

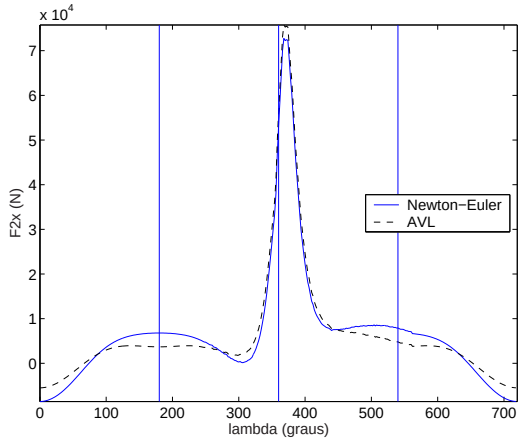

(c) Big end bearing.

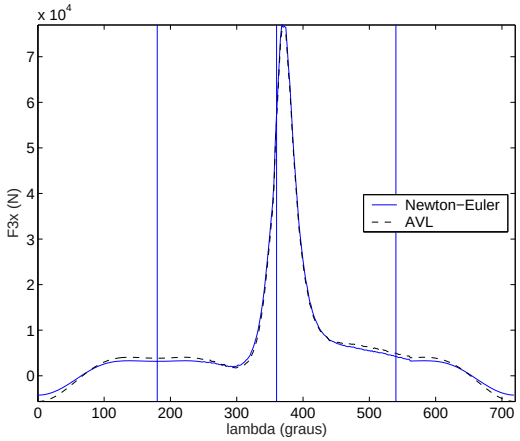

(d) Small end bearing.

Figure 6. Pressure curve and bearing forces in the vertical direction.

6. Conclusions

A dynamic model of the piston-conrod-crank mechanism was presented considering the hydrodynamic bearings. Results were obtained for a pinned system and compared to those ones obtained by the AVL/Excite software. The model presented has a better representation of the inertia forces when compared to the traditional approach. Examples with hydrodynamic bearings have been validated. The dynamic model has been used to study the dynamics of four-stroke engines.

7. References

Affenzeller, J., Gläser, H., 1996,"Lagerung und Schmierung von Verbrennungsmotoren" Springer Verlag.

Bonet, J., Wood, R.D.,1997,"Nonlinear Continuum Mechanics for Finite Element Analisys",Cambridge University Press,Cambridge.

Bonneau, D.,Grente, C.,Garnier, T.,1999,"Three-Dimensional EHD Behavior of the Engine Block/Cranckshaft Assembley for a Four Cylinder Inline Automotive Engine",ASME Journal of Tribology,Vol.121,pp. 721-730.

Gerardin, R.C., 2005, "Dynamic Model of the Piston-Conrod-Crank Mechanism including Hydrodynamic Bearings", Master Thesis, DPM/FEM/UNICAMP.

Ma, Z-D., Perkins, N.C.,2002,"A First Principle Engine Model For Up-Front Design: Further Studies on Hydrodynamic Bearing Models", Proceedings of ASME International Mechanical Engineering Congress and Exposition, New Orleans, Louisiana.

Ma, Z-D., Perkins, N. C.,2003,"An Efficient Multibody Dynamicas Model for Internal COmbustion Engine Systems",Multibody System Dynamics, Kluwer Academic Publishers, Vol.10, pp. 363-391.

Makino, T.,Koga, T.,2002,"Crank Bearing Design Based on 3-D Elasto-hydrodynamioc Lubrication Theory",Mitsubishi Heavy Industries Ltd., Technical Review, Vol.39.

Mendes, A. S., Raminelli, L. F., Gomez, M. P.,2003,"Structural Dimensioning of a Crankshaft for a High Power Diesel Engine", Society of Automotive Engineers, Inc.

Mourelatos, Z.P.,2001,"Crankshaft System Model for Structural Dynamic Analysis of Internal Combustion Engines",Computers & Structures,Vol.79,pp. 2009-2027.

Santos, I.F.,2001,"Dinâmica de Sistemas Mecânicos - Modelagem - Simulação - Visualização - Verificação", Makron, S. Paulo, Brazil.

Wang, D., Keith, T. G., Yang, Q., Vaidyanathan, K.,2004,"Lubrication Analysis of a Connecting-Rod Bearing in a High-Speed Engine. Part II: Lubrication Performance Evaluations for Non-Circular Bearings",Tribology Transactions, Vol. 47, pp. 290-98.

8. Responsibility notice

The author(s) is (are) the only responsible for the printed material included in this paper